International Journal of Biological Sciences
2011; 7(3):333-346

Research Paper

Site-Directed Mutations of Thermostable Direct Hemolysin from *Grimontia hollisae* Alter Its Arrhenius Effect and Biophysical Properties

Yu-Kuo Wang[1*], Sheng-Cih Huang[1*], Yi-Fang Wu[1], Yu-Ching Chen[1], Yen-Ling Lin[1], Manoswini Nayak[1], Yan Ren Lin[1], Wen-Hung Chen[1], Yi-Rong Chiu[1], Thomas Tien-Hsiung Li[2] ✉, Bo-Sou Yeh[3], and Tung-Kung Wu[1] ✉

1. Department of Biological Science and Technology, National Chiao Tung University, 30068, Hsin-Chu, Taiwan, Republic of China
2. Institute of Biochemistry, National Chung Hsing University, 40227, Taichung, Taiwan, Republic of China
3. Hsin Chu General Hospital, Department of Health, Executive Yuan, Taiwan, Republic of China

* These authors contributed equally to this work.

✉ Corresponding author: T. K. Wu, Department of Biological Science and Technology, National Chiao Tung University, 30068, Hsin-Chu, Taiwan, Republic of China. Tel: +886-3-5729287; Fax: +886-3-5725700; E-mail: tkwmll@mail.nctu.edu.tw. T. Li, Institute of Biochemistry, National Chung Hsing University, 40227, Taichung, Taiwan, Republic of China. Tel: +886-4-22840468; E-mail: lithomas@dragon.nchc.edu.tw

Received: 2011.02.13; Accepted: 2011.03.23; Published: 2011.03.31

Abstract

Recombinant thermostable direct hemolysin from *Grimontia hollisae* (Gh-rTDH) exhibits paradoxical Arrhenius effect, where the hemolytic activity is inactivated by heating at 60 °C but is reactivated by additional heating above 80 °C. This study investigated individual or collective mutational effect of Tyr53, Thr59, and Ser63 positions of Gh-rTDH on hemolytic activity, Arrhenius effect, and biophysical properties. In contrast to the Gh-rTDH wild-type (Gh-rTDH^{WT}) protein, a 2-fold decrease of hemolytic activity and alteration of Arrhenius effect could be detected from the Gh-rTDH$^{Y53H/T59I}$ and Gh-rTDH$^{T59I/S63T}$ double-mutants and the Gh-rTDH$^{Y53H/T59I/S63T}$ triple-mutant. Differential scanning calorimetry results showed that the Arrhenius effect-loss and -retaining mutants consistently exhibited higher and lower endothermic transition temperatures, respectively, than that of the Gh-rTDH^{WT}. Circular dichroism measurements of Gh-rTDH^{WT} and Gh-rTDH^{mut} showed a conspicuous change from a β-sheet to α-helix structure around the endothermic transition temperature. Consistent with the observation is the conformational change of the proteins from native globular form into fibrillar form, as determined by Congo red experiments and transmission electron microscopy.

Key words: Grimontia hollisae, thermostable direct hemolysin, Arrhenius effect, Circular Dichroism, virulence factor

Introduction

Grimontia hollisae, formerly described as *Vibrio hollisae*, usually causes moderate gastroenteritis in humans by ingestion of contaminated raw seafood, or contact with the environmental reservoir [1-6]. The pathogen, along with *V. vulnificus*, has been suggested to have a predilection for bloodstream invasion in people with liver abnormalities [2,7]. In addition, the organism can adhere to and invade tissue culture cells [8]. Recently, patients with severe gastroenteritis, hypovolemic shock, bacteremia, and septicemia have been identified with *G. hollisae* infection alone, suggesting a likely underestimation of the incidence of

the *G. hollisae* infection as an invasive disease [8-13].

Thermostable direct hemolysin (TDH) of *Vibrio* species has long been suspected in virulence for bacterial pathogenesis. A major virulence factor of *Vibrio parahaemolyticus* is TDH (Vp-TDH), which is composed of 189 amino acids containing a 24 amino acid signal peptide in the *N*-terminal region and a 165 residue matured peptide in the *C*-terminus region. The TDH of *G. hollisae* (Gh-TDH) is antigenetically and genetically related to that of Vp-TDH [5,14-20]. Previous studies suggested that the Gh-TDH exhibited different heat stability of hemolytic activity compared to that observed for the Vp-TDH, in that Gh-TDH is heat labile, while the Vp-TDH is thermostable after heating for 10 min at 70 or 100 ^{o}C [16]. Moreover, a paradoxical phenomenon known as the Arrhenius effect, whereby the hemolytic activity is inactivated by heating at 60 ^{o}C but is reactivated by additional heating above 80 ^{o}C, was observed for Vp-TDH but not reported for Gh-TDH [21]. These results provoked us to investigate whether the Gh-TDH exhibits a similar Arrhenius effect as that of Vp-TDH. Detailed comparison of the TDH protein sequences from various *G. hollisae* strains revealed a few residues that may be involved in increasing hydrogen bonding, electrostatic interactions, and/or secondary structure and contribute to the enhanced thermostability [22]. In this study, we report the individual or collective mutational effect at positions 53, 59, and 63 on the Arrhenius effect, hemolytic activity, and biophysical properties, based on the sequence differences among various TDHs and their heat stability relative to Vp-TDH [19,21,23]. Our results indicated that amino acid mutations at these positions can alter the protein's Arrhenius effect and hemolytic activity. Furthermore, results from circular dichroism (CD) and differential scanning calorimetry (DSC) experiments showed consistent correlation between conformational change and endothermic transition temperature. Finally, data from transmission electron microscopy and Congo red experiments also supports a model in which conformational changes trap the protein into an aggregated fibrillar form.

Results

Molecular cloning, site-directed mutagenesis, and recombinant production of G. hollisae thermostable direct hemolysin protein

The *Gh-tdh* gene was amplified from *G. hollisae* ATCC 33564 genomic DNA and subcloned into the plasmid pCR®2.1-TOPO to generate the pTOPO-*Gh.tdh* recombinant plasmid. The recombinant pTOPO-*Gh.tdh* plasmid was subjected to protein over-expression and subsequent site-directed mutagenesis. The amino acid residues at positions Tyr53, Thr59, and Ser63 of Gh-TDH were individually or collectively mutated to His53, Ile59, and Thr63, to construct single-, double-, and triple-mutants. The wild-type and mutated *Gh-tdh* genes were separately subcloned into the plasmid pCR®2.1-TOPO, and subsequently transformed into *Escherichia coli* BL21(DE3)(pLysS) cells for proteins over-expression. The PCR®2.1-TOPO plasmid itself, which contained no *tdh* gene insert, was used as a negative control. Following incubation for 16 h at 37 °C, the produced recombinant wild-type and mutated proteins (Gh-rTDHs) were collected, extracted, and subjected to protein purification methods repeatedly using Phenyl-Sepharose 6 Fast Flow columns. Electrophoresis of the purified Gh-rTDHs revealed homogeneous bands at approximate 22 kDa, as determined by sodium dodecyl-polyacrylamide gel electrophoresis (SDS-PAGE) (Fig. 1A). The protein identities of the Gh-rTDHs were also confirmed by MALDI/TOF/TOF mass spectrometry (data not shown). The immunoblot analysis also revealed that both Gh-rTDH wild-type (Gh-rTDH^{WT}) and mutants (Gh-rTDH^{mut}) produced single bands (Fig. 1B). To determine the protein's native state, the Gh-rTDH^{WT} and Gh-rTDH^{mut} proteins were examined using non-denaturing PAGE, showing a single band of approximately 90 kDa (Fig. 1C). Interestingly, the Gh-rTDH$^{Y53H/T59I}$ and Gh-rTDH$^{T59I/S63T}$ double-mutants and the Gh-rTDH$^{Y53H/T59I/S63T}$ triple-mutant migrated slightly faster on the non-denaturing PAGE gel than that of the Gh-rTDH^{WT} and other Gh-rTDH^{mut} proteins. In parallel, the hemolytic activities of Gh-rTDH^{WT} and various Gh-rTDH^{mut} proteins were detected when these proteins were embedded in a blood agar plate (Fig. 1D). For the Gh-rTDH^{WT}, the molecular mass was also detected from the sedimentation coefficient (s) of analytical ultracentrifugation and gel filtration chromatography as 71.3±10.8 and 75 kDa, respectively (Fig. 2A and 2B). Finally, transmission electron microscopy (TEM) analysis of negatively stained Gh-rTDH^{WT} oligomers revealed the presence of particles organized into a square configuration comprised of four smaller particles (Fig. 2C). These results indicated that the Gh-rTDH^{WT} protein exists as a monomer under denatured condition and associates as a homotetramer in solution.

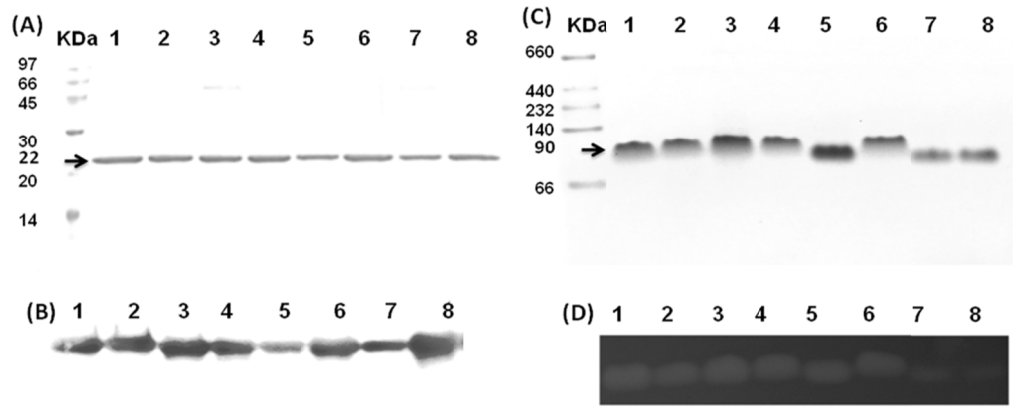

Fig. 1. Purification and identification of the Gh-rTDH^{WT} and Gh-rTDH^{mut} proteins. (A) Coomassie blue-stained SDS-PAGE of Gh-rTDH^{WT} and Gh-rTDH^{mut} proteins with standards. (B) Immunoblot analysis of Gh-rTDH^{WT} and various Gh-rTDH^{mut} proteins with antiserum against Gh-rTDH yielded a single band. (C) Non-denaturing PAGE of Gh-rTDH^{WT} and Gh-rTDH^{mut} proteins with standards. (D) Hemolytic activity detected when the Gh-rTDH^{WT} and Gh-rTDH^{mut} proteins were embedded in a blood agar plate. Lane 1: Phenyl Sepharose 6 Fast Flow purified Gh-rTDH^{WT}; lane 2: Gh-rTDH^{Y53H}; lane 3: Gh-rTDH^{T59I}; lane 4: Gh-rTDH^{S63T}; lane 5: Gh-rTDH$^{Y53H/T59I}$; lane 6: Gh-rTDH$^{Y53H/S63T}$; lane 7: Gh-rTDH$^{T59I/S63T}$; lane 8: Gh-rTDH$^{Y53H/T59I/S63T}$.

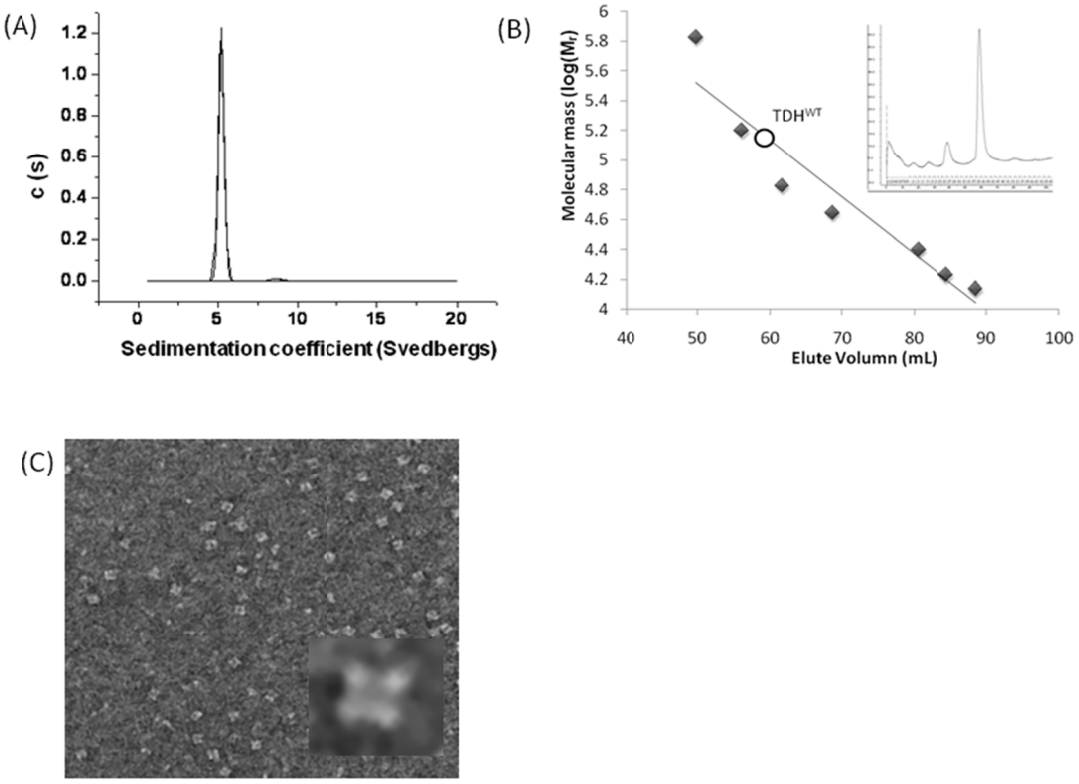

Fig. 2. Preliminary structure of native Gh-rTDH^{WT} protein. (A) Analytical ultracentrifugation determination of the Gh-rTDH^{WT} protein. The calculated molecular mass of Gh-rTDH^{WT} from sedimentation coefficient (s) is approximately 71,255.72 ± 10.83 g/mol. Plot of the distribution of sedimentation coefficients (c(*s*)) vs. S, where S is plotted in Svedberg units, calculated from the concentration profiles. (B) Gel filtration chromatography estimated molecular mass of Gh-rTDH^{WT} protein (open circle). The figure shows the migration positions of the Gh-rTDH^{WT} protein in comparison with the standard proteins used to calibrate the column. Closed diamonds indicate molecular mass standards: thyroglobulin (670 kDa), γ-globulin (158 kDa), albumin (66 kDa), ovalbumin (44 kDa), chymotrypsinogen A (25 kDa), myoglobulin (17 kDa), ribonuclease A (14 kDa). The inset shows the gel filtration analysis of Gh-rTDH^{WT}. (C) Representative electron microscopic image of negatively stained native form of Gh-rTDH^{WT}. The inset shows the image obtained by single-particle analysis.

Hemolytic activity and thermostability determination of Gh-rTDHWT and Gh-rTDHmut proteins

To investigate whether the individual or collective amino acid substitutions at positions 53, 59, and 63 on the Arrhenius effect for the hemolytic activity, each of the expressed proteins was incubated at different temperatures ranging from 4 to 100 °C for 30 min. Following heat incubation at different temperatures, the protein solution was cooled down to 37 °C by two different means followed by analysis of hemolytic activity. The first was rapid cooling by inserting the reaction tube into an ice bath. The second was by gradually decreasing the temperature by putting the reaction tube in the air.

We first analyzed the mutational effect of Gh-rTDH proteins at 37 °C for hemolytic activity. Figure 3 shows the percentage of hemolysis as a function of the Gh-rTDH protein concentration. The Gh-rTDH^{WT} protein exhibited 50% hemolytic activity at 2 μg/mL concentration. We then analyzed the individual or collective mutational effect of Tyr53, Thr59, and Ser63 of Gh-rTDH for hemolytic activity. Interestingly, the Gh-rTDH^{Y53H} mutant exhibited similar activity as that observed for the Gh-rTDH^{WT} protein, while the Gh-rTDH^{T59I}, Gh-rTDH^{S63T} and Gh-rTDH$^{Y53H/S63T}$ mutants demonstrated approximately 2-4-folds increased activity. Alternatively, the Gh-rTDH$^{Y53H/T59I}$, Gh-rTDH$^{T59I/S63T}$, and Gh-rTDH$^{Y53H/T59I/S63T}$ mutants showed a 2-fold reduction in hemolytic activity than that observed for Gh-rTDH^{WT}.

We then analyzed the mutational effect of Gh-rTDH proteins incubated at different temperatures and subsequently cooled down to 37 °C for hemolytic activity. Interestingly, when Gh-rTDH^{WT} was incubated at a temperature below 55 °C for 30 min, no apparent activity loss was observed (Fig. 4A, column 3-10). However, incubation of Gh-rTDH^{WT} protein at 60-80 °C for 30 min followed by rapidly cooling to 37 °C resulted in a hemolytic activity of only 8.1±1.6% (Fig. 4A, column 11-15). Furthermore, after a 30 min incubation at 85-100 °C and rapidly cooled to 37 °C, the Gh-rTDH^{WT} recovered 64.7-72.6±5% of its original hemolytic activity (Fig. 4A, column 16-19). On the contrary, the hemolytic activity declined to only 7.4±1.3% when the Gh-rTDH^{WT} was incubated at 95 °C followed by slow cooling to 37 °C (data not shown). Next, each of the Gh-TDH^{mut} mutants was incubated at 37, 70 and 90 °C for 30 min, followed by rapid cooling, and then subjected to Arrhenius effect determination of the hemolytic activity. When the abovementioned mutants were incubated at 37 °C for 30 min, no apparent activity loss was observed (Fig. 4B).

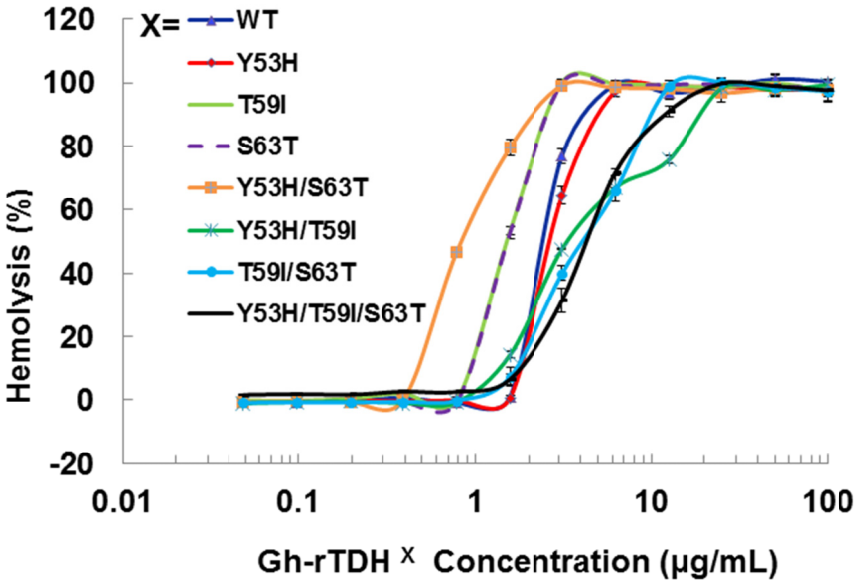

Fig. 3. Titration of hemolytic activity of human red blood cells by the Gh-rTDH^{WT} and Gh-rTDH^{mut} proteins. Hemolysis was assessed by turbidity at room temperature using an automated microplate reader. The final percentage of hemolysis was calculated as described in the experimental procedures section. Data points shown are mean ± S.D. for three independent experiments.

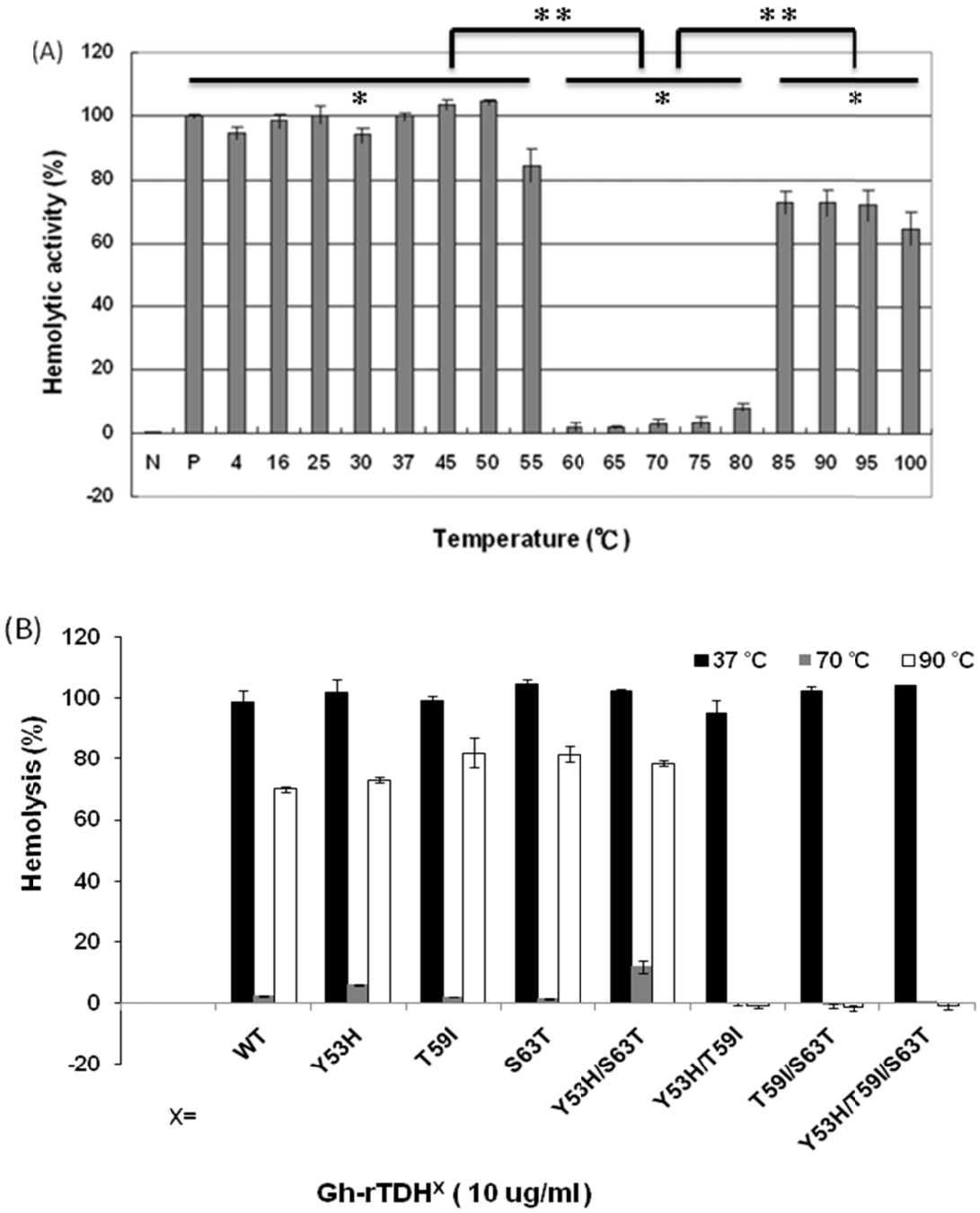

Fig. 4. Arrhenius effect assay of Gh-rTDH^{WT} and Gh-rTDH^{mut} proteins. (A) Relative hemolytic activity of Gh-rTDH^{WT}, measured at 37°C after various heat treatment from 4 to 100 °C for 30 min. *: not significant; **: Statistically significant ($p<0.05$). Statistically significant ($p < 0.05$ between 4-55, 60-80 and 85-100 °C). Not significant in 4-55, 60-80 and 85-100 °C. (B) Relative hemolytic activity of Gh-rTDH$^{Y53X/T59X/S63X}$ individual or collective mutants, measured at 37 °C after heat treatment at 37, 70, and 90 °C for 30 min followed by rapid cooling to 37 °C. Statistically significant ($p < 0.05$ between various mutants protein in 90 °C). Not significant between various mutants protein in 37 and 70 °C. Relative hemolytic activities were measured after various treatments (n = 3 per group). N, negative control (PBS buffer); P, positive control (0.1% Triton X-100).

Surprisingly, incubation of Gh-rTDH^{mut} proteins at 70 and 90 °C, respectively, for 30 min followed by rapid cooling to 37 °C resulted in the loss of hemolytic activity for Gh-rTDH$^{Y53H/T59I}$, Gh-rTDH$^{T59I/S63T}$, and Gh-rTDH$^{Y53H/T59I/S63T}$ mutants, while the rest of the mutants retained approximately 70% hemolytic activity (Fig. 4B). These results indicated that the Gh-rTDH^{WT} exhibits Arrhenius effect similar to that of Vp-TDH, which is inactivated when heated at 60 °C but can be reactivated by additional heating above 80 °C and subsequently rapid cooled to 37 °C. Furthermore, although a single mutation on Thr59 of Gh-rTDH did not affect the hemolytic activity and Arrhenius effect, collective mutations of the double and triple mutants involved Thr59 caused the decline of the hemolytic activity and alteration of the Arrhenius effect.

Differential scanning calorimetry assay of Gh-rTDH heat stability

In 2005, Fukui et al. reported the detoxification and transformation of Vp-TDH into nontoxic fibrils rich in β-strands by incubation at 60 °C [21]. We next investigated the individual or collective mutational effect on protein thermal stability, using differential scanning calorimetry (DSC) to determine the specific heats of the Gh-rTDH^{WT} and Gh-rTDH^{mut} proteins, respectively. Figure 5 shows the plot of heat capacity *Cp* vs. temperature for Gh-rTDH^{WT} and various Gh-rTDH^{mut} proteins. Endothermic transitions at T_m = 58.4, 58.0, 57.1, 56.6, 56.3, 55.3, 52.0, and 51.8 °C and heat capacities of 23.66, 36.53, 34.59, 52.61, 65.48, 65.71, 18.16, 22.45 kcal/K.mol, were determined for Gh-rTDH$^{Y53H/T59I/S63T}$, Gh-rTDH$^{Y53H/T59I}$, Gh-rTDH$^{T59I/S63T}$, Gh-rTDH^{WT}, Gh-rTDH$^{Y53H/S63T}$, Gh-rTDH^{S63T}, Gh-rTDH^{Y53H}, and Gh-rTDH^{T59I} proteins, respectively. Surprisingly, the mutants with a transition temperature above the Gh-rTDH^{WT}, which is at 56.6 °C, conform to alteration of the Arrhenius effect by heating at 70 and 90 °C. Since the general properties of the substituted amino acid side chains at these positions are similar, the difference observed in the Arrhenius effect may be due to a conformational trap at the Gh-rTDH fibrillar state formation.

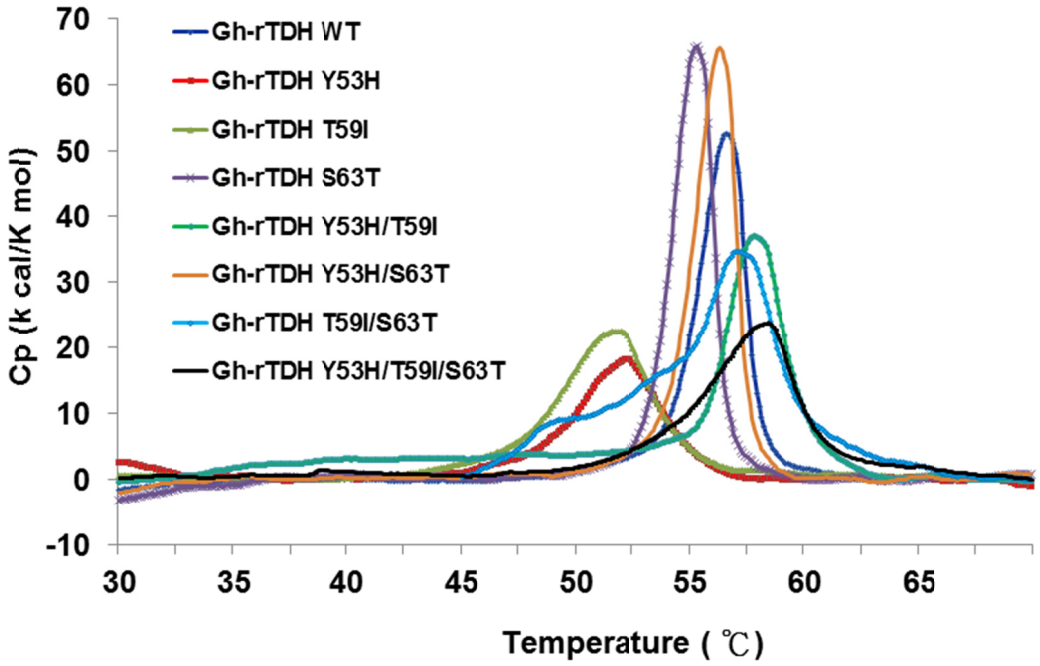

Fig. 5. Differential scanning calorimetry scans of Gh-rTDH^{WT} and Gh-rTDH^{mut} proteins. Shown are the profiles of heat capacity (*Cp*) vs. temperature at a scan rate of 0.5 °C/min for Gh-rTDH^{WT} and Gh-rTDH^{mut} proteins.

Circular Dichroism of Gh-rTDHs reveals conformational change

To investigate the mutational effect on the secondary structure of the protein, far-UV CD spectra (190-250 nm) of Gh-rTDH^{WT}, Gh-rTDH$^{Y53H/T59I}$, Gh-rTDH$^{T59I/S63T}$, and Gh-rTDH$^{Y53H/T59I/S63T}$ mutants, were determined at different temperatures. As shown in Fig. 6 and supplement Table 1, at temperatures below 55 °C, the Gh-rTDH^{WT}, Gh-rTDH$^{Y53H/T59I}$, Gh-rTDH$^{T59I/S63T}$, and Gh-rTDH$^{Y53H/T59I/S63T}$ all showed similar far-UV CD spectra with nearly identical negative elliptical peaks minimum at ~218 nm, characteristic of protein containing predominantly β-sheet structures. Nevertheless, when the temperature was increased from 55 to 80 °C, the far-UV CD spectra changed from positive to negative absorbance at 202 nm, indicating the secondary structure change from β-sheet to α-helix for all measured proteins. Specifically, the CD spectrum of Gh-rTDH^{WT} changed at 55 °C while those of the Gh-rTDH^{muts} (Gh-rTDH$^{Y53H/T59I}$, Gh-rTDH$^{T59I/S63T}$, and Gh-rTDH$^{Y53H/T59I/S63T}$) changed when the temperature was increased to 60 °C, indicating the pronounced difference in the Gh-rTDH^{WT} and Gh-rTDH^{mut} proteins for their secondary structure stability. Furthermore, the Gh-rTDH^{WT} and the Gh-rTDH^{mut} (Gh-rTDH$^{Y53H/T59I}$, Gh-rTDH$^{T59I/S63T}$ and Gh-rTDH$^{Y53H/T59I/S63T}$) proteins completed the secondary structure change by 70 and 80 °C, respectively.

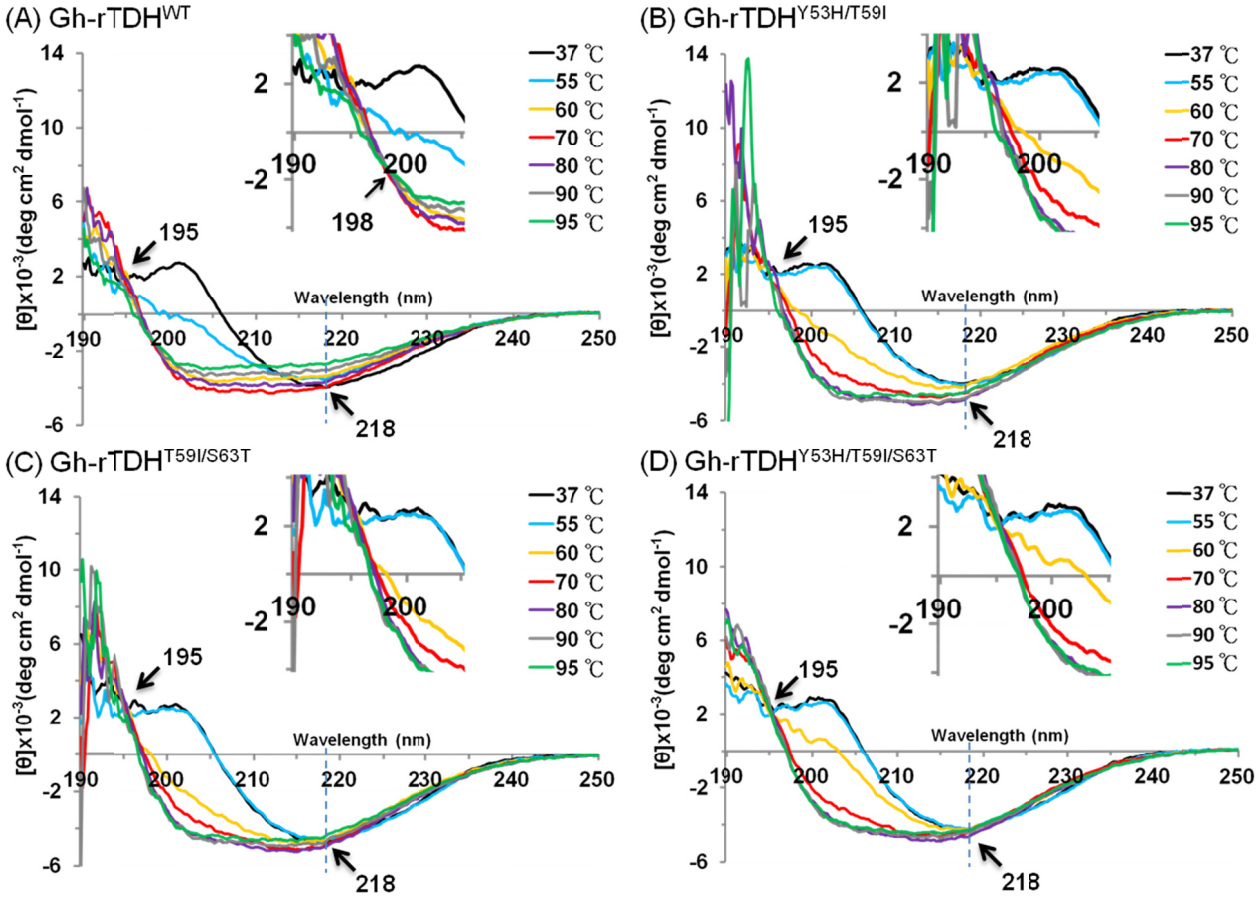

Fig. 6. Temperature dependence of the far-UV CD spectra of (A) Gh-rTDH^{WT}, (B) Gh-rTDH$^{Y53H/T59I}$, (C) Gh-rTDH$^{Y53H/T59I}$ and (D) Gh-rTDH$^{Y53H/T59I/S63T}$ proteins in 10 mM phosphate buffer (pH 7.0) at 37, 55, 60, 70 °C. The arrows at 195 and 218 nm indicate the isodichroic points and the negative maximal peak, respectively. The arrow at 198 nm within the inset shows the second isodichroic point of Gh-rTDH^{WT} protein.

Consistent with the observation is that no further change at 201 nm could be detected for Gh-rTDH^{WT} protein at 70 °C, while a further increase of the negative ellipticity at 201 nm absorbance could be detected for those of Gh-rTDH$^{Y53H/T59I}$, Gh-rTDH$^{T59I/S63T}$, and Gh-rTDH$^{Y53H/T59I/S63T}$ mutants at temperatures above 70 °C. In parallel, an isodichroic point at 195 nm was observed for both the Gh-rTDH^{WT} and all the Gh-rTDH^{mut} proteins, supporting a two-state transition for all measured proteins between 55 and 80 °C. Further increasing the temperature from 70 to 95 °C, a decrease of the absolute ellipticity in the far-UV region was observed for Gh-rTDH^{WT}, characteristic of the secondary structure change into an unfolded state. However, at temperatures above 80 °C, the Gh-rTDH$^{Y53H/T59I}$, Gh-rTDH$^{T59I/S63T}$ and Gh-rTDH$^{Y53H/T59I/S63T}$ proteins exhibited distinct CD spectra from that of the Gh-rTDH^{WT}, which no apparent change of the absolute ellipticity could be observed for Gh-rTDH$^{Y53H/T59I}$, Gh-rTDH$^{T59I/S63T}$ and Gh-rTDH$^{Y53H/T59I/S63T}$. A second isodichroic point at 198 nm could be detected for the Gh-rTDH^{WT} but not for Gh-rTDH^{mut} proteins, indicating a second two-state transition occurred specifically for Gh-rTDH^{WT} (Fig. 6A inset). These results suggest that the Gh-rTDH proteins exhibit the first secondary structure change generally for both the Gh-rTDH^{WT} and the Gh-rTDH$^{Y53H/T59I}$, Gh-rTDH$^{T59I/S63T}$ and Gh-rTDH$^{Y53H/T59I/S63T}$ proteins around the endothermic transition temperature, and exhibit the second secondary structure change specifically for the Gh-rTDH^{WT} at temperature above 70 °C. Therefore, at least three states, a native state below the endothermic transition temperature, an intermediate state at 55-70 °C, and an unfolded state above 80 °C, could be detected for the heat-induced transitions of the Gh-rTDH^{WT} protein. Conversely, perhaps a two-state but not a three-state transition occurred for the Gh-rTDH$^{Y53H/T59I}$, Gh-rTDH$^{T59I/S63T}$ and Gh-rTDH$^{Y53H/T59I/S63T}$ proteins, which the amino acid mutation within the Gh-rTDH^{WT} that causes the loss of the Arrhenius effect.

Inhibitory effects of Congo red on Gh-rTDHWT hemolytic activity and fibril formation

Hemolytic activity analysis revealed that the paradoxical Arrhenius effect of the Vp-TDH protein is related to structural changes in the protein that produce fibrils [21]. Previously, inhibitory effect on red blood cell hemolysis and a characteristic red shift in absorbance spectrum were observed when Congo red bound to native amyloidogenic proteins and amyloid fibrils, respectively [28,29]. A dose-dependent inhibitory effect of Congo red was also observed on Vp-TDH hemolysis [21]. We then investigated the effect of accumulation of Congo red to the inhibition of Gh-rTDH^{WT} hemolytic activity and its absorbance spectrum on binding to Gh-rTDH^{WT} fibrils. The results showed that Gh-rTDH^{WT} hemolysis is inhibited by Congo red in a dose-dependent manner (Fig. 7A). The IC_{50} for Congo red inhibition on Gh-rTDH hemolysis was approximately 11 μM. To investigate the effect of Congo red binding on absorbance wavelength shift, apo-myoglobin (apo-Mb), native Gh-rTDH^{WT} and heat-treated Gh-rTDH^{WT}, respectively, were incubated with Congo red and the corresponding absorbance spectra were measured. The negative control, the α-helix rich apo-Mb, exhibited a characteristic absorbance increase with only a slight red shift. In addition, the native Gh-rTDH^{WT} also exhibited an absorbance increase but not a red shift. On the contrary, a characteristic absorbance increase with a clear red shift (495 to 527 nm) could be detected for the heat-treated Gh-rTDH^{WT} (Fig. 7B). Consistent with the observation is the detection of Gh-rTDH^{WT} fibrils from the TEM assay after heat treatment (Fig. 7C). These results indicated that Congo red can bind to the native Gh-rTDH^{WT} and inhibit the hemolytic activity as well as cause a red shift in the absorbance spectrum when the protein produces fibrils.

Discussion

The number of reports on the connection between *G. hollisae* infection and patients with severe gastroenteritis diseases is increasing. In addition, the characterization of virulence factors responsible for pathogenesis is a prerequisite for future development of targeted drug therapy. In this study herein, we have characterized the mutational effect of Gh-rTDH on the Arrhenius effect, hemolytic activity and biophysical properties. Recently, Hamada *et al.* reported that the Vp-TDH protein possesses a tetrameric and a monomeric structure in aqueous solvents and high salt concentrations, respectively; whereas the protein transforms into nontoxic fibrils rich in β-strands by incubations at 60 °C [21,40]. Similarly, the expressed Gh-TDH^{WT} protein exists as a monomer under denatured condition and associates into a homotetramer in solution. In addition, the Gh-rTDH^{WT} protein can be transformed into nontoxic fibrils when incubated between 60 and 80 °C, as shown by the Congo red and TEM results. The Gh-rTDH^{WT} fibrils incubated above 80 °C dissociate into an unfolded state, which can refold into the toxic Gh-rTDH^{WT} native form upon rapid cooling to 37 °C. These phenomena are consistent with the Arrhenius effect, in which the protein is detoxified by heating at 60-80 °C but reactivated by additional heating above 85 °C.

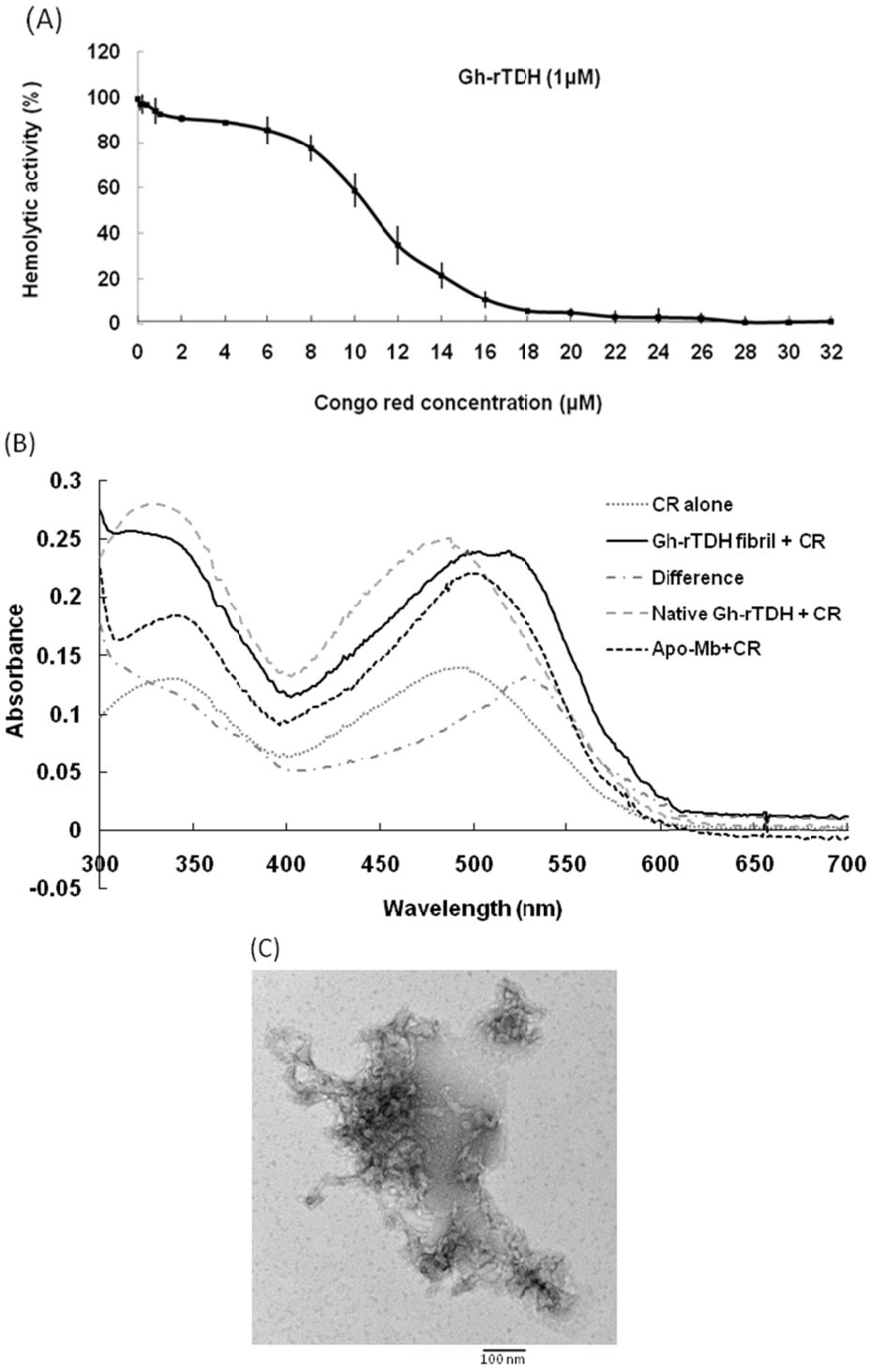

Fig. 7. Effect of Congo red on the Gh-rTDH^{WT} protein. (A) Dose-dependent inhibition of Congo red on the Gh-rTDH^{WT} hemolysis. Various concentrations of Congo red were pre-incubated with 1 M Gh-rTDH^{WT} for 30 min, subsequently incubated with human 4% (v/v) erythrocytes for 30 min, and the viability of the cells were determined by the hemolytic activity assay. The data are means ± S.D. from at least three independent experiments. (B) Absorbance spectra of a Congo red solution in the absence or presence of native Gh-rTDH^{WT} and Gh-rTDH^{WT} fibrils, respectively. The α-helix rich apo-Mb was used as a negative control. The difference spectrum is obtained by subtracting the Congo red spectrum in the absence of Gh-rTDH^{WT} fibrils from the corrected Congo red spectrum in the presence of Gh-rTDH^{WT} fibrils. (C) Representative transmission electron microscopic image of the Gh-rTDH^{WT} fibrils form after heat treatment.

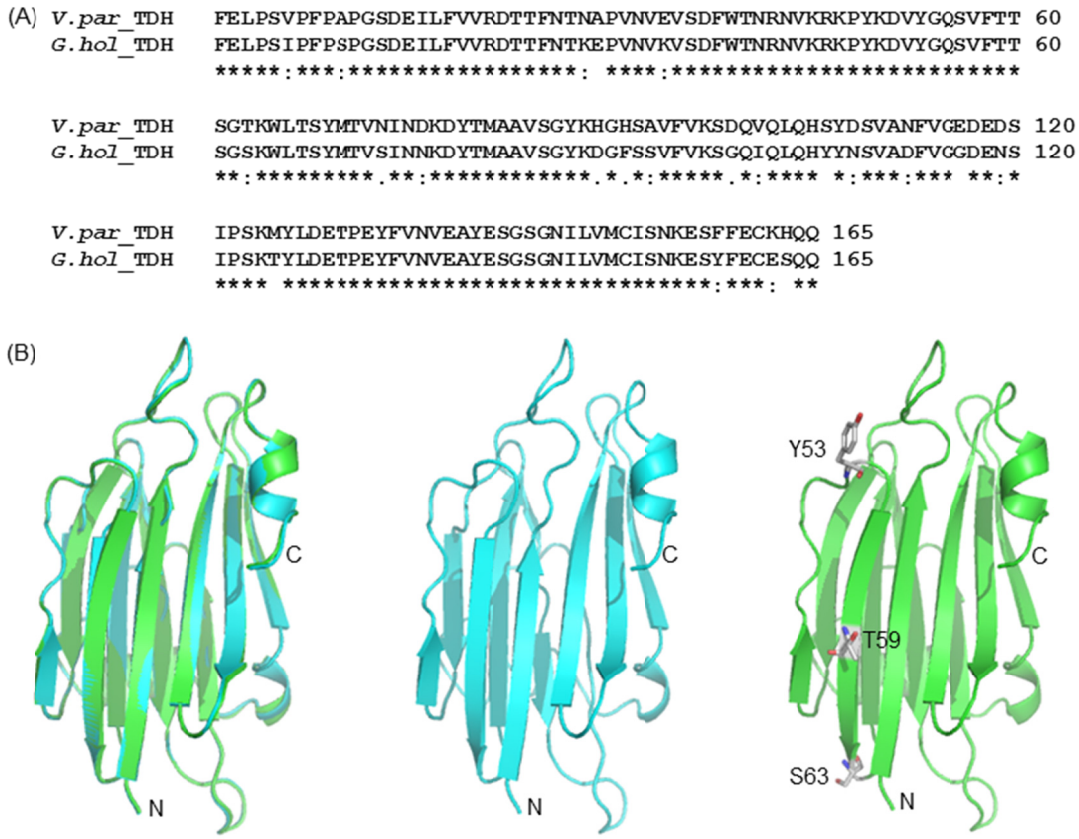

Fig. 8. (A) Amino acid sequence alignment of *G.hollisae* TDH and *V. parahaemolyticus* TDH2. (B) The structural model of the *G.hollisae* TDH showing with cartoon view. The two structures were overlaid using the PyMol software. Superposition of the Vp-TDH (blue) and the Gh-TDH (green) structures. The *N*- and *C*-terminal ends as well as the Y53, T59, and S63 residues of the protein are indicated.

Therefore, the over-expressed Gh-rTDH^{WT} is highly homologous to the Vp-TDH but differs in thermostability from the previously purified Gh-TDH by Yoh *et al.* [16]. Conceivably, the discrepancies could be due to different experimental conditions, including differences in the cooling rate used, since Yoh et al. performed the heat stability experiments at only 70 and 100 ^{o}C, and no detailed experimental procedures were provided [16].

Both the Vp-TDH and Gh-rTDH^{WT} proteins showed characteristics that the native form exhibits hemolytic activity and Congo red inhibitory effect, whereas the fibril form displays no hemolytic activity and an absorbance increase with a clear red shift. Proteins associated with Alzheimer's disease, type II diabetes, primary and secondary systemic amyloidosis, and the spongiform encephalopathies such as Creutzfeldt-Jakob disease have been known to be related to the formation of fibrils [28,30,31]. However, a range of proteins not associated with any diseases and many amyloidogenic proteins with little amino acid homology can also form amyloid fibrils. The SH3 domain of bovine phosphatidyl-inositol-3'-kinase and the N-terminal domain of the *E. coli* HypF protein can aggregate *in vitro* into fibrils indistinguishable from those found in pathological conditions and appear to be inherently harmless to cells, which are consistent with our results that the heat-treated Gh-rTDH fibrils exhibit no hemolytic activity [32]. Therefore, the amyloid formation may be a generic property of the polypeptide chain in various conditions [33-36].

To elucidate the mutational effect on the alteration of Arrhenius effect, we generated the Gh-rTDH homology model, based on the Vp-TDH crystal structure (Fig. 8) [37]. The Gh-rTDH protein homology model indicated that Tyr53 and Ser63 are located at both ends of a β-sheet, whereas Thr59 is positioned in the middle of the β-sheet structure [37]. According to the Chou-Fasman rules for secondary structure

prediction, individual substitution of Tyr53 to His, Thr59 to Ile, or Ser63 to Thr does affect the β-sheet probability [38]. However, collective mutations at positions 53 and 59, 59 and 63, or simultaneously included 53, 59 and 63, may disrupt the secondary structure or tertiary structure. Consistent with the prediction is the difference observed in far-UV CD spectra for Gh-rTDH$^{Y53H/T59I}$ and Gh-rTDH$^{T59I/S63T}$ double-mutants and the Gh-rTDH$^{Y53H/T59I/S63T}$ triple-mutant (Fig. 6).

The CD properties difference of Gh-rTDH^{WT}, Gh-rTDH$^{Y53H/T59I}$ and Gh-rTDH$^{T59I/S63T}$, and Gh-rTDH$^{Y53H/T59I/S63T}$ can potentially explain the alteration of the Arrhenius effect. CD analysis showed that Gh-rTDH^{WT} could interconvert among at least three conformational states, depending on the temperature; while two states were identified for Gh-rTDH$^{Y53H/T59I}$, Gh-rTDH$^{T59I/S63T}$ and Gh-rTDH$^{Y53H/T59I/S63T}$ mutants. A decrease of CD spectrum at 201 nm was observed when the temperature was increased above 60 °C, indicating the destruction of β-sheet and the accumulation of α-helical intermediates. Similarly, Hamada et al. also reported accumulation of α-helical intermediates during the unfolding of β-lactoglobulin, a predominantly β-sheet protein, supporting our observations [39]. Subsequently, Gh-rTDH^{WT} fibrils incubated over 80 °C dissociate into unfolded states, which refold into native form upon rapid cooling to 37 °C. Conversely, the Gh-rTDH$^{Y53H/T59I}$, Gh-rTDH$^{T59I/S63T}$ and Gh-rTDH$^{Y53H/T59I/S63T}$ fibrils retained the secondary structures when incubated over 80 °C and showed no hemolytic activity when cooled to 37 °C, consistent with an alteration of the Arrhenius effect. Furthermore, CD and DSC results of Gh-rTDH^{WT}, Gh-rTDH$^{Y53H/T59I}$, Gh-rTDH$^{T59I/S63T}$, and Gh-rTDH$^{Y53H/T59I/S63T}$ showed close correlation between conformational change and their endothermic transition temperatures. Consistent with this observation is that a mutationally-induced increase of the endothermic transition temperature caused the alteration of the Arrhenius effect and the heat-induced fibril development of Gh-rTDH^{WT} and Gh-rTDH$^{Y53H/T59I/S63T}$ when incubated around 55 °C and 60 °C, respectively.

In summary, a TDH protein from *G. hollisae* was successfully produced, and amino acid residues putatively involved in affecting Arrhenius effect, hemolytic activity, and biophysical properties were identified. The Gh-rTDH$^{Y53H/T59I}$, Gh-rTDH$^{T59I/S63T}$ and Gh-rTDH$^{Y53H/T59I/S63T}$ mutants can alter the protein's Arrhenius effect and hemolytic activity. Furthermore, consistent correlation of conformational changes from β-sheet to α-helix and subsequent aggregation into fibrillar form to the endothermic transition temperature were also observed from CD, DSC, TEM and Congo red experiments. Further studies to elucidate the physiological and structural characteristics of Gh-rTDH^{WT} and related mutants are warranted.

Materials and methods

Bacterial strains and materials

The *G. hollisae* strain ATCC 33564 was obtained in a freeze-dried form from the Culture Collection and Research Center (Hsin-Chu, Taiwan). This bacterium showed hemolysis on tryptic soy broth (TSB) agar plates containing 1.5% NaCl and 5% sheep blood. Phenyl Sepharose 6 Fast Flow and protein molecular weight standards were purchased from GE Healthcare (Piscataway, NJ). The protein assay kit was obtained from Bio-Rad (Hercules, CA). Protein purification chemicals were obtained from Calbiochem (La Jolla, CA).

Grimontia hollisae thermostable direct hemolysin: Cloning, expression, purification, and preparation of monoclonal antibodies

The cloning, expression, purification, preparation and characterization of monoclonal antibodies of Gh-rTDH^{WT} were performed according to the previous report [24,25]. Site-directed mutations of Tyr53, Thr59, and Ser63 in the *G. hollisae tdh* wild-type gene were performed using the QuikChange site-directed mutagenesis kit (Stratagene Inc., La Jolla, CA). The oligonucleotide primers used are shown in Table 1. Mutations were confirmed by DNA sequencing. The recombinant plasmids were electroporated into the *E. coli* BL21(DE3)(pLysS) cells, and read for loss or decrease of hemolytic activity for growth on 5% sheep blood agar plates.

Assay for hemolytic activity and thermostability of the *G. hollisae* TDH

Hemolytic activity was assayed according to a previously described method with rabbit erythrocytes that were washed three times with the 100 mM phosphate-buffered saline (PBS) (pH 7.6) and resuspended at a concentration of 4% (v/v) [25]. For the hemolytic activity assays, 0.1 mL of 0.1% Triton X-100, which causes complete release of hemoglobin from erythrocytes and results in the maximum change in absorbance at 540 nm, was used as a positive control. The elution buffers, which caused negligible erythrocyte hemolysis compared with sample fractions, were used as negative controls. The effect of temperature on the hemolytic activity of purified TDH was determined by incubating 1 μM of the purified protein in PBS for 30 min at different temperatures (4, 16, 25, 30,

37, 45, 50, 55, 60, 65, 70, 75, 80, 85, 90, 95, 100 °C), rapidly equilibrated at 37 °C, and then assayed for the residual hemolytic activity with 4% rabbit erythrocytes.

Table 1. Primer sequences used for mutagenesis.

tdh gene	Template (*tdh* gene in pCR®2.1-TOPO)	PCR primer sequence
tdh^{Y53H}	tdh^{WT}	F 5'-TgTgAAgACTgATTgTCCgTGAACATCTTT-3' R 5'-AAAgATgTTCACggACAATCAgTCTTCACA-3'
tdh^{T59I}	$tdh^{Y53H/T59I}$	F 5'-TgTgAAgACTgATTgTCCATAAACATCTTTgTA-3' R 5'-TACAAAgATgTTTATggACAATCAgTCTTCACA-3'
tdh^{S63T}	$tdh^{Y53H/S63T}$	F 5'-TgTgAAgACTgATTgTCCATAAACATCTTTgTA-3' R 5'-TACAAAgATgTTTATggACAATCAgTCTTCACA-3'
$tdh^{Y53H/T59I}$	$tdh^{Y53H/T59I/S63T}$	F 5'-ggATgTTAACCATTTAgAACCTgACgTTAT-3' R 5'-ATAACgTCAggTTCTAAATggTTAACATCC-3'
$tdh^{Y53H/S63T}$	$tdh^{Y53H/T59I/S63T}$	F 5'-AgTACCTgACgTTgTgAAgACTgATTgTCC-3' R 5'-ggACAATCAgTCTTCACAACgTCAggTACT-3'
$tdh^{T59I/S63T}$	tdh^{WT}	F 5'-TTTAgTACCTgACgTTATgAAgACTgATTgTCC-3' R 5'-ggACAATCAgTCTTCATAACgTCAggTACTAAA-3'
$tdh^{Y53H/T59I/S63T}$	tdh^{Y53H}	F 5'-TTTAgTACCTgACgTTATgAAgACTgATTgTCC-3' R 5'-ggACAATCAgTCTTCATAACgTCAggTACTAAA-3'

Protein electrophoresis and detection

For sodium dodecylacrylamide gel electrophoresis (SDS-PAGE), the protein sample was mixed with 5X sample treatment buffer (125 mM Tris-HCl, pH 6.8, 2% SDS, 10% glycerol, 5% β-merceptoethanol, and 0.05% bromophenol blue), and heated at 100 °C for 10 min. For native PAGE, the protein was mixed with the above-mentioned buffer prepared without 5% β-merceptoethanol, 2% SDS, and heating. Electrophoresis was performed according to the manufacturer's instructions. After electrophoresis, the gel was soaked in Coomassie Blue R 250 staining solution for 20 min, then the gel was destained with destaining solution I (40% methanol, 7% acetic acid) and II (5% methanol, 7% acetic acid) until the stained band was distinct against a clear background. The native PAGE gel was embedded onto the agar plate containing 5% sheep erythrocytes and incubated at 37 °C for 1 hr.

In western blotting experiments, proteins were electrophoretically separated and transferred onto polyvinylidene difluoride (PVDF) membranes. The PVDF membranes were washed by the PBS buffer (pH 7.6) containing 0.05% Tween 20 (PBST) for 10 min, and immunodetection was carried out by following the procedure for the ECL western blotting system, using monoclonal antibody raised against the TDH (1:500) and anti-mouse immunoglobulin HRP-peroxidase conjugate (1:5000). Excess ligand was washed away with PBS for 30 min, and detection of the proteins was performed according to the manufacturer's instructions (Amersham Pharmacia Biotech, Piscataway, NJ, USA). The membrane was exposed to Hyperfilm ECL for different times or until a suitable signal was obtained.

Analytical ultracentrifugation analysis

An analytical ultracentrifugation method developed by Stafford was applied to characterize the solution-state, especially the subunit stoichiometries, of the Gh-rTDH protein [26]. To describe briefly, 500 μL of the Gh-rTDH protein equilibrated in the 20 mM Tris-HCl pH 7.2 was subjected to analytical ultracentrifugation in order to obtain an apparent distribution of sedimentation coefficients, c(s), and the determined apparent molecular mass. In addition, 500 μL of the buffer alone was used as reference control to the reference sector.

Differential scanning calorimetry (DSC)

Differential scanning calorimetry (DSC) is used to investigate protein stability, and is combined with other biophysical methods to link thermodynamics, structure, and function [27]. Calorimetric measurements were performed using the DSC-Q10 (TA instruments, New Castle, DE). The DSC-Q10 was run

without feedback and 15-30 min equilibration times at 30 °C were used before or between scans. Protein samples were concentrated to 0.8 mg/mL in a 10 mM phosphate buffer, pH 7.2. The proteins were scanned from 25 °C to 90 °C at a heating rate of 0.5 °C /min. A pan containing 10 mM phosphate buffer at pH 7.2 was used as a reference. DSC data was corrected for instrument base lines and normalized for scan rate and protein concentration. Data obtained for TDH protein were analyzed with the TA advantage specialty Lib program. Excess heat capacity (C_p) is expressed as kilocalories per Kelvin per mole, where 1.000 cal = 4.184 J. All experiments were done in duplicate.

Circular dichroism (CD)

CD spectra were recorded with a J-815 spectropolarimeter (JASCO, Tokyo, Japan) equipped with a thermoelectric temperature controller. The heat-induced conformational transitions of Gh-rTDH were evaluated by measuring the ellipticity from 190 to 300 nm. Measurements were taken in a quartz cuvette with a path length of 1 mm, scanned in steps of 1 nm at a rate of 50 nm/min. The data from 6 runs were averaged. Samples of 0.18 mg/mL Gh-rTDH wild-type and mutants in 10 mM phosphate buffer at pH 7.0 were used for experiments. The protein concentrations were 0.5 mg/mL for measurements of far- and near-UV CD spectra. CD measurements were carried out in a temperature range of 25-95 °C with the increment of 5 or 1 °C (50-90 °C). Samples were pre-incubated at desired temperatures for 5 min before CD measurements. The raw CD data at a given wavelength, λ were converted into mean residue ellipticity, $[\theta]_\lambda$ (expressed in deg cm^2 dmol^{-1}) using the relation,

$$[\theta]_\lambda = \frac{\theta_\lambda M_0}{10lc}$$

Where $[\theta]_\lambda$ is the observed ellipticity in millidegrees at wavelength λ, M_0 is the mean residue weight of the protein, c is the protein concentration (mg/cm^3), and l is the path length of the cell (cm). Data were processed with software provided by JASCO. The experiments were repeated three times.

Congo red effect of *G. hollisae* TDH

Congo red was assayed for inhibitory effect on TDH hemolysis activity. Various concentrations of Congo red (0 to 32 μM at the intervals of 2 μM) were preincubated with 1 μM of Gh-rTDH for 30 min. Then the Gh-rTDH solution, with or without Congo red, was incubated in 4% (v/v) rabbit erythrocyte with a total volume of 200 μL for 30 min at 37 °C. For hemolytic activity assays, UV absorbance at 540 nm was measured as above-mentioned. Binding experiments were performed as following: firstly, various concentrations of CR (5-50 μM) were incubated with 100 μg/mL of Gh-rTDH in fibril form. Mixtures of CR and fibrils were incubated at room temperature for 1 h prior to spectral analysis. The absorbance spectra from 300 to 700 nm were recorded for the CR-fibril mixture, as well as the CR and fibril alone at the appropriate concentrations. The instrument was blanked with the PBS buffer. All reactions were carried out in triplicate.

Acknowledgements

We thank National Chiao Tung University and Ministry of Education, Aiming for Top University Plan (MOE ATU Plan), and the National Science Council (NSC-97-2627-M-009-003 and NSC-99-2113-M-009 -004 -MY2) for financially supporting this research. We are grateful to Mr. Justin Moses for his comments. We thank the National Center for High-Performance Computing for running the protein modeling jobs. We also thank Prof. Chia-Ching Chang and Mr. Hsueh-Liang Chu (Department of Biological Science and Technology, National Chiao Tung University) for their assistance.

Abbreviations

Gh-TDH: *Grimontia hollisae* thermostable direct hemolysin; Vp-TDH: *Vibrio parahaemolyticus* thermostable direct hemolysin; DSC: differential scanning calorimetry; CD: circular dichroism.

Conflict of Interests

The authors have declared that no conflict of interest exists.

References

1. Hickman FW, Farmer JJ 3rd, Hollis DG, Fanning GR, Steigerwalt AG, Weaver RE, and Brenner DJ. Identification of *Vibrio hollisae* sp. nov. from patients with diarrhea. J Clin Microbiol. 1982; 15: 395-401
2. Morris JG Jr., Miller HG, Wilson R, Tacket CO, Hollis DG, Hickman FW, Weaver RE, and Blake PA. Illness caused by *Vibrio damsela* and *Vibrio hollisae*. Lancet 1982; 1: 1294-1297
3. Lowry PW, McFarland LM, and Threefoot HK. *Vibro hollisae* septicemia after consumption of catfish. J. Infect. Dis. 1986; 154: 730-731
4. Kelly MT, and Stroh EM. Occurrence of *Vibrionaceae* in natural and cultivated oyster populations in the Pacific Northwest. Diagn. Microbiol. Infect. Dis. 1988; 9: 1-5
5. Nishibuchi M, Doke S, Toizumi S, Umeda T, Yoh M, and Miwatani T. Isolation from a coastal fish of *Vibrio hollisae* capable of producing a hemolysin similar to the thermostable direct hemolysin of *Vibrio parahaemolyticus*. Appl. Environ. Microbiol. 1988; 54: 2144-2146

6. Thompson FL, Hoste B, Vandemeulebroecke K, and Swings J. Reclassification of *Vibrio hollisae* as *Grimontia hollisae* gen. nov., comb. nov.. Int J Syst Evol Microbiol. 2003; 53: 1615-1617
7. Tilton RC, and Ryan RW. Clinical and ecological characteristics of *Vibrio vulnificus* in the northeastern United States. Diagn. Microbiol. Infect. Dis. 1987; 6: 109-117
8. Miliotis MD, Tall BD, and Gray RT. Adherence to and invasion of tissue culture cells by *Vibrio hollisae*. Infect. Immun. 1995; 63: 4959-4963
9. Abbott SL, and Janda JM. Severe gastroenteritis associated with *Vibrio hollisae* infection: report of two cases and review. Clin. Infect. Dis. 1994; 18: 310-312
10. Carnahan AM, Harding J, Watsky D, and Hansman S. Identification of *Vibrio hollisae* associated with severe gastroenteritis after consumption of raw oysters. J. Clin. Microbiol. 1994; 32: 1805-1806
11. Gras-Rouzet S, Donnio PY, Juguet F, Plessis P, Minet J, and Avril JL. First European case of gastroenteritis and bacteremia due to *Vibrio hollisae*. Eur. J. Clin. Microbiol. Infect. Dis. 1996; 15: 864-866
12. Lesmana M, Subekti DS, Tjaniadi P, Simanjuntak CH, Punjabi NH, Campbell JR, and Oyofo BA. Spectrum of vibrio species associated with acute diarrhea in North Jakarta, Indonesia. Diagn. Microbiol. Infect. Dis. 2002; 43: 91-97
13. Hinestrosa F, Madeira RG, and Bourbeau PP. Severe gastroenteritis and hypovolemic shock caused by *Grimontia (Vibrio) hollisae* infection. J. Clin. Microbiol. 2007; 45: 3462-3463
14. Kothary MH, and Richardson SH. Fluid accumulation in infant mice caused by *Vibrio hollisae* and its extracellular enterotoxin. Infect. Immun. 1987; 55: 626-630
15. Kothary MH, Claverie EF, Miliotis MD, Madden JM., and Richardson SH. Purification and characterization of a Chinese hamster ovary cell elongation factor of *Vibrio hollisae*. Infect. Immun. 1995; 63: 2418-2423
16. Yoh M, Honda T, and Miwatani T. Purification and partial characterization of a *Vibrio hollisae* hemolysin that relates to the thermostable direct hemolysin of a *Vibrio parahaemolyticus*. Can. J. Microbiol. 1986; 32: 632-636
17. Honda T, Ni Y, Yoh M, and Miwatani T. Evidence of immunologic cross-reactivity between hemolysins of *Vibrio hollisae* and *Vibrio parahaemolyticus* demonstrated by monoclonal antibodies. J. Infect. Dis. 1989; 160: 1089-1090
18. Yoh M, Honda T, and Miwatani T. Homogeneity of a hemolysin(Vh-rTDH) produced by clinical and environmental isolates of *Vibrio hollisae*. FEMS Microbiol. Lett. 1989; 52: 171-175
19. Yamasaki S, Shirai H, Takeda Y, and Nishibuchi M. Analysis of the gene of *Vibrio hollisae* encoding the hemolysin similar to the thermostable direct hemolysin of *Vibrio parahaemolyticus*. FEMS Microbiol. Lett. 1991; 64: 259-263
20. Nishibuchi M, Janda JM, and Ezaki T. The thermostable direct hemolysin gene (tdh) of *Vibrio hollisae* is dissimilar in prevalence to and phylogenetically distant from the tdh genes of other vibrios: implications in the horizontal transfer of the tdh gene. Microbiol. Immunol. 1996; 40: 59-65
21. Fukui T, Shiraki K, Hamada D, Hara K, Miyata T, Fujiwara S, Mayanagi K, Yanagihara K, Iida T, Fukusaki E, Imanaka T, Honda T, and Yanagihara I. Thermostable direct hemolysin of *Vibrio parahaemolyticus* is a bacterial reversible amyloid toxin. Biochemistry 2005; 44: 9825-9832
22. Vogt G, Woell S, and Argos P. Protein thermal stability, hydrogen bonds, and ion pairs. J. Mol. Biol. 1997; 269: 631-643
23. Yoh M, Honda T, Miwatani T, Tsunasawa S, and Sakiyama F. Comparative amino acid sequence analysis of hemolysins produced by *Vibrio hollisae* and *Vibrio parahaemolyticus*. J. Bacteriol. 1989; 171: 6859-6861
24. Wang YK, Huang SC, Wu YF, Chen YC, Chen WH, Lin YL, Nayak M, Lin YR, Li TTH., and Wu TK. Purification, crystallization, and preliminary X-ray analysis of a Thermostable Direct Hemolysin from *Grimontia hollisae*. Acta Crystallogr. Sect. F 2011; 67: 224-227
25. Wu TK, Wang YK, Chen YC, Feng JM, Liu YH, and Wang TY. Identification of a *Vibrio furnissii* oligopeptide permease and characterization of its in vitro hemolytic activity. J. Bacteriol. 2007; 189: 8215-8223
26. Tang GQ, Iida T, Inoue H, Yutsudo M, Yamamoto K, and Honda T. A mutant cell line resistant to *Vibrio parahaemolyticus* thermostable direct hemolysin (TDH): its potential in identification of putative receptor for TDH. Biochim. Biophys. Acta, 1997; 1360: 277-282
27. Freire E. The thermodynamic linkage between protein structure, stability, and function. Methods Mol. Biol. 2001; 168: 37-68
28. Mattson MP, Begley JG, Mark RJ, and Furukawa K. Abeta25-35 induces rapid lysis of red blood cells: contrast with Abeta1-42 and examination of underlying mechanisms. Brain Res. 1997; 771: 147-153
29. Klunk WE, Jacob RF, and Mason RP. Quantifying amyloid beta-peptide (Abeta) aggregation using the Congo red-Abeta (CR-abeta) spectrophotometric assay. Anal. Biochem. 1999; 266: 66-76
30. McLaurin J, and Chakrabartty A. Membrane disruption by Alzheimer beta-amyloid peptides mediated through specific binding to either phospholipids or gangliosides. Implications for neurotoxicity. J Biol Chem. 1996; 271: 26482-26489
31. Kelly JW. Structure and association of ATP-binding cassette transporter nucleotide-binding domains. Nat. Struct. Biol. 2002; 9: 323-325
32. Bucciantini M, Giannoni E, Chiti F, Baroni F, Formigli L, Zurdo J, Taddei N, Ramponi G, Dobson CM, and Stefani M. Inherent toxicity of aggregates implies a common mechanism for protein misfolding diseases. Nature 2002; 416: 507-511
33. Chiti F, Bucciantini M, Capanni C, Taddei N, Dobson CM, and Stefani M. Solution conditions can promote formation of either amyloid protofilaments or mature fibrils from the HypF N-terminal domain. Protein Sci. 2001; 10: 2541-2547
34. Chiti F, Taddei N, Bucciantini M, White P, Ramponi G, and Dobson CM. Mutational analysis of the propensity for amyloid formation by a globular protein. EMBO J. 2000; 19: 1441-1449
35. Chiti F, Webster P, Taddei N, Clark A, Stefani M, Ramponi G, and Dobson CM. Designing conditions for in vitro formation of amyloid protofilaments and fibrils. Proc. Natl. Acad. Sci. USA 1999; 96: 3590-3594
36. Guijarro JI, Sunde M, Jones JA, Campbell ID, and Dobson CM. Amyloid fibril formation by an SH3 domain. Proc. Natl. Acad. Sci. USA 1998; 95: 4224-4228
37. Yanagihara I, Nakahira K, Yamane T, Kaieda S, Mayanagi K, Hamada D, Fukui T, Ohnishi K, Kajiyama S, Shimizu T, Sato M, Ikegami T, Ikeguchi M, Honda T, and Hashimoto H. Structure and functional characterization of *Vibrio parahaemolyticus* thermostable direct hemolysin (TDH). J. Biol. Chem. 2010; 285: 16267-16274
38. Chou PY, and Fasman GD. Prediction of the secondary structure of proteins from their amino acid sequence. Adv. Enzymol. Relat. Areas Mol. Biol. 1978; 47: 45-148
39. Hamada D, Segawa S, and Goto Y. Non-native alpha-helical intermediate in the refolding of beta-lactoglobulin, a predominantly beta-sheet protein. Nat. Struct. Biol. 1996; **3**: 868-873
40. Hamada D, Higurashi T, Mayanagi K, Miyata T, Fukui T, Iida T, Honda T, and Yanagihara I. Tetrameric structure of thermostable direct hemolysin from Vibrio parahaemolyticus revealed by ultracentrifugation, small-angle X-ray scattering and electron microscopy. J Mol. Biol. 2007; **365**:187-195